

Regularization-based Pruning of Irrelevant Weights in Deep Neural Architectures

Giovanni Bonetta^{1*}, Matteo Ribero¹ and Rossella Cancelliere¹

¹Computer Science Department, University of Turin, Via Pessinetto, Turin, 10149, Italy.

*Corresponding author(s). E-mail(s): giovanni.bonetta@unito.it;

Contributing authors: matteo.ribero@edu.unito.it; rossella.cancelliere@unito.it;

Abstract

Deep neural networks exploiting millions of parameters are nowadays the norm in deep learning applications. This is a potential issue because of the great amount of computational resources needed for training, and of the possible loss of generalization performance of overparametrized networks. We propose in this paper a method for learning sparse neural topologies via a regularization technique which identifies non relevant weights and selectively shrinks their norm, while performing a classic update for relevant ones. This technique, which is an improvement of classical weight decay, is based on the definition of a regularization term which can be added to any loss functional regardless of its form, resulting in a unified general framework exploitable in many different contexts. The actual elimination of parameters identified as irrelevant is handled by an iterative pruning algorithm. We tested the proposed technique on different image classification and Natural language generation tasks, obtaining results on par or better than competitors in terms of sparsity and metrics, while achieving strong models compression.

Keywords: Sparsity, Pruning, Regularization, NLP, Image Processing

1 Introduction

Deep learning models have constantly established in the past few years new state-of-the-art performances in a flood of different domains, including image processing [1–5], image captioning [6, 7], language generation [8–11], and machine translation [12, 13].

The resources required to properly train them however can be prohibitive, since the number of weights used for these tasks may easily sum up to several millions. These growing performance costs have therefore induced scientists to look for techniques limiting the size of neural architecture parameters.

An effective approach for reducing this complexity is sparsity, defined as the property that

a substantial subset of the model parameters have a value of zero (i.e. layers’ weights matrices are sparse). Sparsity allows smaller computational and storage requirements and, as shown for example in [14] and [15], deep architectures tolerate it well. It can reduce the memory footprint of regular networks to fit mobile devices, as well as shorten training time. Besides, sparsity is also a solution for improving inference performance through overfitting control and, as suggested by [16], it may lead to improved performance in transfer learning scenarios.

Numerous methods for inducing sparsity have been proposed over the past few years: a non-exhaustive review can be found in Section 2.

Among the most popular ones the L_2 regularization based techniques, detailed in Section 3, add a penalty term to the cost functional in order to shrink parameters' values. All parameters dropping below a predefined threshold are then set to zero, thus obtaining sparse architectures.

A drawback of these methods is that neural weights' norms are all driven close to zero without taking account of weight relevance in the neural architecture, as discussed in detail in [17, 18].

Our work relies on this approach: we propose a new loss functional holding a suited regularization term which is a specialization of the well-known weight decay. It allows to derive a new weights' update rule which selectively decreases the norm of non relevant weights, while performing a classic update for relevant ones. Weights' update directly follows from loss optimization, not requiring the definition of ad hoc update rules, as frequently done (see [14, 17–19]). Shrunk weights are then pruned in order to sparsify the neural architecture.

Our technique is general, as the proposed regularization term can be added to any loss functional regardless of its form, and constitutes a unified framework potentially exploitable for many different applications.

We verify the effectiveness of our method in the context of image classification and natural language generation, respectively sparsifying convolutional and self-attention based neural architectures; while the former task has already been addressed in literature, it is still rare to find sparsity techniques applied to language generation architectures.

We reach state-of-the-art results in two out of four image classification tasks, while establishing, at the best of our knowledge, new state-of-the-art performance for the others and for the considered language generation tasks.

The rest of this paper is organized as follows: Sections 2 contains an overview of related works. In Section 3 the theoretical foundations of our model are presented and Section 4 outlines the details of our pruning algorithm. Sections 5 and 6 describe datasets, implementation details and results obtained in both contexts.

2 Related works

Among the earliest approaches to sparsity that can be found in literature, methods based on

merely removing small norm weights are the simplest ones [14, 20].

Methods grounded in Bayesian statistics constitute another possibility to achieve sparsity: Soft Weight Sharing (SWS) approach [15] succeeds in reducing the number of parameters to be stored, sharing the redundant ones among layers. Weights are represented as a mixture of gaussian distributions, where the components of the mixture are learned.

Sparse Variational Dropout [21] treats dropout as noise applied to the inputs of all neural layers; it represents the first attempt to use dropout technique for sparsifying networks, paving the way for new research in the field (see for instance [22]). Targeted Dropout [19] is another dropout-based approach, which focus on disentangling important subset of weights from unimportant ones in order to get stable pruning. Before computing the gradients for each weight update, targeted dropout stochastically selects a set of units or weights to be dropped, using L1 and L2 norm as a proxy for weight importance, and then computes the gradients for the remaining weights.

The authors of SNIP [23] define a saliency-based criterion on network's connections to select the most important ones for the given task. Then they prune the network accordingly in a one-shot way and finally train the model to get good accuracy. The drawback of this algorithm is that its one-shot nature prevent it to achieve sparsity level comparable to iterative approaches.

Guo et al. attempted to address this issue proposing the DNS [24] technique, where the incorrectly pruned connections could be re-established by a splicing pass if evaluated important, making the pruning effort dynamic.

As stated in Section 1, regularization can be used as a particularly effective shrink-and-prune approach to sparsity [25] but with the drawback that all weights are indiscriminately penalized.

An effective way to avoid this issue is presented in [17], where the idea of output-based sensitivity is introduced: weights are selectively penalized depending on their capability to induce variations on network outputs when changed. A refinement of this method is presented in [18], where state-of-the-art results are reached in image classification thanks to the introduction of loss-based sensitivity, which aims at shrinking weights which are contributing the least to the final loss value.

3 The relevance-based pruning method: theory

Regularization methods turn an original unstable, ill-posed problem into a well-posed one [27]; they limit the capacity of models by adding a parameter norm penalty to the loss functional L , to control overfitting and decrease the test error (see [28]).

One of the most common parameter norm penalty is $L2$, commonly known as Tikhonov regularization [29, 30], ridge regression or weight decay.

In a neural context, the regularized loss \tilde{L} depends on each weight $w_{i,j}^n$ belonging to layer n and connecting neurons i and j , and has the form:

$$\tilde{L}(\bar{w}) = L(\bar{w}) + \lambda \|\bar{w}\|^2 = L(\bar{w}) + \lambda \sum_{n,i,j} \|w_{i,j}^n\|^2 \quad (1)$$

where \bar{w} is the vector whose elements are $w_{i,j}^n$ and λ is the regularization parameter. The iterative application of stochastic gradient descent algorithm (SGD) at time step t

$$w_{i,j}^n(t) \equiv w_{i,j}^n(t-1) - \eta \frac{\partial \tilde{L}(\bar{w})}{\partial w_{i,j}^n} \quad (2)$$

results in the well known weights' decay update rule

$$w_{i,j}^n(t) = w_{i,j}^n(t-1) - \eta \frac{\partial L(\bar{w})}{\partial w_{i,j}^n} - 2\lambda w_{i,j}^n \quad (3)$$

where η is the learning rate. The neural weights therefore are driven close to zero without taking account of their relevance in the neural architecture.

The main contribution of this work is the proposal of a new loss functional \hat{L} , modified with respect to eq. (1), allowing to get a new selective weight decay rule which shrinks the magnitude of only those weights which are not relevant to the final error. We propose to modify the regularization term in eq. (1) multiplying it by a coefficient which measures how much the final loss value is influenced by modification of $w_{i,j}^n$.

The quantity $|\frac{\partial L}{\partial w_{i,j}^n}|$ would seem to be a good candidate for this: small derivative values for example indicate that even a large variation of

$w_{i,j}^n$ do not cause large loss variations, i.e. weight changes are not relevant to the final loss value. In addition, large derivative values are not interesting because they characterize relevant weights and we aim at driving to zero (and prune) only irrelevant ones. This derivative anyway is not upper bounded, which is a possible issue in order to preserve convergence properties.

Taking account of these requests we therefore define the *coefficient of irrelevance* $I_{n,i,j}$ as:

$$I_{n,i,j} \equiv \exp(-|\frac{\partial L}{\partial w_{i,j}^n}|), \quad 0 < I_{n,i,j} < 1. \quad (4)$$

$I_{n,i,j}$ is bounded and assumes values near 1 for irrelevant weights and near 0 for relevant ones. Moreover it has the useful property to be almost everywhere differentiable.

We can now define the new loss functional \hat{L} , modified with respect to eq. (1) to selectively limit the magnitude of weights:

$$\begin{aligned} \hat{L}(\bar{w}) &\equiv L(\bar{w}) + \lambda \sum_{n,i,j} (I_{n,i,j} \cdot |w_{i,j}^n|^2) = \\ &= L(\bar{w}) + \lambda \sum_{n,i,j} (\exp(-|\frac{\partial L}{\partial w_{i,j}^n}|) \cdot |w_{i,j}^n|^2) \end{aligned} \quad (5)$$

The iterative application of stochastic gradient descent algorithm to \hat{L} allows to derive the new weights' update rule:

$$\begin{aligned} w_{i,j}^n(t) &\equiv w_{i,j}^n(t-1) - \eta \frac{\partial \hat{L}}{\partial w_{i,j}^n} = \\ &= w_{i,j}^n(t-1) - \eta \frac{\partial L}{\partial w_{i,j}^n} - 2\eta\lambda \exp(-|\frac{\partial L}{\partial w_{i,j}^n}|) w_{i,j}^n \\ &\quad - \eta\lambda |w_{i,j}^n|^2 \cdot \exp(-|\frac{\partial L}{\partial w_{i,j}^n}|) (-1) \frac{\partial}{\partial w_{i,j}^n} |\frac{\partial L}{\partial w_{i,j}^n}| = \\ &= w_{i,j}^n(t-1) - \eta \frac{\partial L}{\partial w_{i,j}^n} - 2\eta\lambda \exp(-|\frac{\partial L}{\partial w_{i,j}^n}|) w_{i,j}^n \\ &\quad + \eta\lambda |w_{i,j}^n|^2 \cdot \exp(-|\frac{\partial L}{\partial w_{i,j}^n}|) \operatorname{sgn}(|\frac{\partial^2 L}{\partial w_{i,j}^n{}^2}|) \end{aligned} \quad (6)$$

As usually done in first order derivative optimization methods, we can neglect the second-order derivative term, so that eq. (6) becomes:

$$w_{i,j}^n(t) = w_{i,j}^n(t-1) - \eta \frac{\partial L}{\partial w_{i,j}^n} - 2\eta\lambda \exp\left(-\left|\frac{\partial L}{\partial w_{i,j}^n}\right|\right) w_{i,j}^n \quad (7)$$

Different weights' updates are made in the two cases determined by the extreme values of I :

- $I \sim 0$: in this case the weight is relevant. The third term in eq. (7) is roughly zero, so a classic update is performed, without targeted reduction of weight norm.
- $I \sim 1$: in this case the weight is irrelevant. Because $I \sim 1$ implies $\frac{\partial L}{\partial w_{i,j}^n} \sim 0$, the second term in eq. (7) is roughly zero, and the update rule becomes:

$$w_{i,j}^n(t) \simeq w_{i,j}^n(t-1) - 2\eta\lambda w_{i,j}^n \quad (8)$$

We can see that in this case the weight is actually driven to zero at each iteration, because if $w_{i,j}^n > 0$ then $\Delta w_{i,j}^n < 0$ (i.e. the norm of a positive irrelevant weight is decreased); on the other hand, if $w_{i,j}^n < 0$ then $\Delta w_{i,j}^n > 0$.

4 Pruning algorithm description

The pruning algorithm proceeds this way:

1. We get a checkpoint to finetune from. A common choice is to either find it in literature or train it on our own. Another possibility is to use a randomly initialized checkpoint.
2. We finetune the checkpoint (or train it from scratch when starting from a random initialization) by using our proposed regularization term, as in equation (5). In this step any optimizer can be used. During finetuning we regularly evaluate the model performances on the validation set, and:
 - **prune**. If the validation performance is higher than a user-defined *lower-bound*, a fixed percentage (*pruning-percentage*) of the remaining model parameters is pruned, choosing from the ones with lower magnitude.
 - **not prune**. If the validation performance is lower than the user-defined lower-bound, the model is not ready to be pruned, so the finetuning proceeds normally.

3. These last two steps of the finetuning process are iteratively repeated until the model reaches a validation performance plateau (so it can not be pruned further).
4. We perform a final finetuning phase without regularization, aiming to get the best performing checkpoint.

When advanced in training, usually the model reaches an accuracy plateau making difficult for the algorithm to hit a pruning step. Because of this we introduce an exponential decay schedule on λ which decreases the regularization term between two validation step. This procedure favours accuracy with respect to sparsification and helps the model to break the performance plateau and to cross over the lower bound leading to further pruning.

Some hyperparameters are needed to implement this process:

- *evaluation-interval*: number of steps between two validation performance assessments.
- *lower-bound*: performance lower-bound. For the image classification task the performance is measured by accuracy, while for the language generation task we use BLEU [31]. The lower-bound is chosen as slightly lower than the state-of-the-art performance.
- *pruning-percentage*: The percentage of remaining non-zero parameters to be pruned at every pruning step.

If not stated otherwise, hyperparameters are chosen via grid-search both in training and finetuning phases.

We made all our experiments using one Nvidia TITAN RTX 24Gb GPU and we will make our code available upon acceptance.

5 Imaging

We test our method on four different image classification datasets chosen among the most popular benchmarks in literature for sparsity research. Each of them has been processed using architectures producing state-of-the-art performance.

Table 1 Hyperparameters used in imaging experiments.

Hyperparameters	LeNet	ResNet32	VGG16
# epochs	120	290	30
# batch size	100	128	100
η	0.001	0.0005	0.0001
Optimizer	Adam	SGD	SGD
lower-bound	98.7	92.9	68.5
λ	0.001	1e-6	1e-4
pruning-percentage	4 %	4 %	1 %
eval-interval	250	25	2500

5.1 Dataset Description

MNIST

MNIST [32], is composed of 70,000 28x28 grey-scale images containing handwritten numbers; the database is split into training set (60,000 images) and test set (10,000 images).

Fashion-MNIST

Fashion-MNIST [33], based on the assortment of Zalando’s website, is a dataset comprising of 28x28 grayscale images of 70,000 fashion products from 10 categories, with 7,000 images per category. Like MNIST, the training set has 60,000 samples and the test set 10,000. Fashion-MNIST, although similar to MNIST, is more challenging.

CIFAR-10

CIFAR-10 [34], from the Canadian Institute for Advanced Research, is a subset of the Tiny Images dataset [35] and consists of 60,000 32x32 color images labelled with one of 10 mutually exclusive classes: airplane, automobile, bird, cat, deer, dog, frog, horse, ship, and truck. There are 6000 samples per class, split in 5000 for training and 1000 for testing.

ImageNet

ImageNet [36] is arranged according to the WordNet [37] noun hierarchy and is a real image database, in which each node of the hierarchy is represented by thousands of images; it contains more than 20,000 categories. In total, 14 million pictures were hand-annotated and for one million of those the bounding boxes were also provided. The RGB images have an average size of 469x387 pixels, but are usually preprocessed by sampling them at 256x256 pixels.

5.2 LeNet-5 on MNIST

This network [38] consists of a Convolution (Conv) layer with 6 5x5 filters, a 2x2 Pooling layer, a Convolution layer with 10 5x5 filters, another 2x2 Pooling Layer and three fully connected (FC) layers (120, 84, 10), for a total of 431080 parameters.

Since MNIST is an easy dataset, a pretrained checkpoint is not necessary, so we directly trained with regularization from scratch, using hyperparameter values resumed in table 1. Finally we finetuned without regularization for 5 additional epochs. Results from our model and competitors are shown in table 2, together with the performance of the not sparsified baseline model.

Performances on MNIST are very similar to each other since accuracy and sparsification on this simple task have reached the top possible ones, i.e. very close to 100 %. With our method we obtain less than 1,5k non zero residual weights, a result primarily due to a better sparsification of the fully connected layers, where the majority of the weights are. We obtain almost the best accuracy with the only exception of Sparse VD even though with higher sparsity. We also note that we get the same result of Han et al. but with 8% less weights.

5.3 LeNet-5 on Fashion-MNIST

We obtain the initial checkpoint after training for 21 epochs. We then use the same hyperparameters shown in table 1, except for lower-bound = 90.5 and epochs = 75, for finetuning with regularization; finally we finetune without regularization for 50 additional epochs. Table 3 compares performances on this dataset.

As we can see our method reaches the best performance both in terms of accuracy and compression.

5.4 ResNet32 on CIFAR-10

This model [3] is composed of a Convolution layer with 16 3x3 filters, a batch normalization layer, 3 ResNet layers and a final dense layer, for a total of 464,154 trainable parameters. All the ResNet layers are composed of 5 ResNet blocks, with different configuration: they all share 2 Batch Normalization layers, but differ in the number of kernels generated by the 2 Convolutional layers (16 3x3 filters for the blocks of the first ResNet layer, 32

Table 2 Test results for LeNet-5 architecture on MNIST dataset.

Methods	Residual Weights (%)				Accuracy (%)	Sparsity (%)
	Conv1	Conv2	FC1	FC2		
Baseline	100	100	100	100	99.32	–
Han et al., 2015 [14]	66	12	8	19	99.23	91.59
Tart. et al., 2018 [17]	67.6	11.8	0.9	31.0	99.22	98.04
DNS [24]	14	3	0.7	4	99.09	99.09
SWS [15]	-	-	-	-	99.03	99.38
Tart. et al., 2021 [18]	22	2.38	0.22	5.98	99.21	99.56
L0 [26]	45	36	0.4	5	99.00	98.57
Sparse VD [21]	33	2	0.2	5	99.25	99.64
Our method	29	1.82	0.11	3.35	99.23	99.71

Table 3 LeNet-5 on Fashion-MNIST.

Methods	Residual Weights (%)				Accuracy (%)	Sparsity (%)
	Conv1	Conv2	FC1	FC2		
Baseline	100	100	100	100	91.90	–
Tart. et al., 2018 [17]	76.2	32.56	6.5	44.02	91.50	91.48
Han et al., 2015 [14]	-	-	-	-	91.56	93.04
Tart. et al., 2021 [18]	78.6	26.13	2.88	32.66	91.53	95.70
Our method	78.84	17.84	1.20	6.26	91.70	97.66

3x3 for the second ResNet layer and 64 3x3 for the third ResNet layer). The initial checkpoint is obtained with the hyperparameters shown in table 1 training for 200 epochs with $\eta = 0.1$. After finetuning with regularization, we finetune without it for 1 last epoch with a batch size = 64 and $\eta = 6e-5$.

Table 4 show that our technique on this more challenging task, which involves a deeper neural architecture and real images, outperforms in terms of sparsity all competitors. With respect to accuracy, both our method and Tartaglione et al. reach the baseline values.

5.5 VGG-16 on ImageNet

The model is composed by 13 Convolutional layers with 3x3 filters followed by Relu activations. These layers are interleaved by 5 MaxPooling layers. Finally an AdaptiveAveragePool layer with 7x7 dimension is used before a sequence of 3 Linear layers with Relu activations which lead to the 1000-dimensional output. The model consists of 138,357,544 parameters and for our experiment we

Table 4 ResNet-32 on CIFAR-10.

Methods	Accuracy (%)	Sparsity (%)
Baseline	92.67	–
Sparse VD [21]	92.12	50.11
L0 [26]	91.20	60.00
Han et al., 2015 [14]	91.92	71.51
Targeted Dropout [19]	92.54	80.00
Tart. et al., 2021 [18]	92.67	80.11
Our method	92.67	81.27

start our regularized finetuning from a pretrained checkpoint¹ using the hyperparameters shown in table 1. We further finetune for 30 epochs without regularization to get the best accuracy.

Results show that VGG-16 is highly overparameterized for the task, since all methods are able to prune almost 93% of the network’s parameters, shrinking them from ~ 138 M to less than 10M. Our method confirms its ability to scale to a bigger

¹<https://pytorch.org/vision/stable/index.html>

Table 5 VGG-16 on ImageNet.

Method	Residual Weights (%)		Accuracy (%)	Sparsity (%)
	Convolutional	FC		
Baseline	100	100	71.30	–
Han et al., 2015 [14]	32.77	4.61	68.66	92.49
Tart. et al., 2018 [17]	56.49	2.56	69.08	92.91
Our model	37.48	3.57	69.48	92.82

model (~ 100 M weights) obtaining the best accuracy among the shown methods with a sparsity percentage very close to the best one.

6 Language Generation

The first studies concerning sparsity in language architectures appeared recently [21, 25], following the progressive replacing of recurrent architectures by transformer based models, and mainly focused on attention heads pruning [39, 40]. Nonetheless, with respect to the great amount of available sparsity techniques for imaging, it is yet rare to find as many results in the context of language generation.

We tried to fill this gap sparsifying the Transformer [12] on two different language tasks: dialog learning and machine translation. We implemented the model using the Huggingface² library which provides easy access to different datasets, tokenizers and output generation techniques. Since our sparsification algorithm is not architecture-specific, no modifications are needed with respect to what described in Sec. 4.

6.1 Dataset Description

WMT14

WMT14 [42] is a collection of datasets presented in the Ninth Workshop on Statistical Machine Translation. It comes as a parallel corpus made by sentences translated in various languages. It is derived from many different sources, among which there are the Europarl corpus [43] (created from the European Parliament Proceedings in the official languages of the EU), the News Commentary [44] corpus and the Common Crawl corpus [45] (which was collected from web sources).

For our experiments we use the English to German translation dataset En-De WMT14, provided by the Stanford Natural Language Processing Group [46], which is more than 300x bigger than the Taskmaster-1; it contains 4,468,840 training samples and 3000 test samples. Some source-translation examples is shown in table 6.

Taskmaster-1

Taskmaster-1 [41] is a public crowdsourced dataset, released by Google in 2019, where Amazon turkers were asked to write dyadic dialogs (see table 7) following some given set of instructions describing six tasks: ordering pizza, creating auto repair appointments, setting up rides for hire, ordering movie tickets, ordering coffee drinks and making restaurant reservations. The dataset is composed of 13,215 task-based dialogs (12,355 for the training set and 770 for the test set), including 5,507 spoken and 7,708 written dialogs.

6.2 Transformer on WMT14

Transformer architecture details are described in table 8 and follow the settings from [25].

In order to obtain the initial checkpoint, we train the model for 10 epochs with batch size = 120, $\eta = 5e - 05$, using Adam optimizer ($\beta_1 = 0.85, \beta_2 = 0.997, eps = 1e - 8$) and reach comparable BLEU performance with the baseline defined in [25].

Starting from the checkpoint described above, the finetuning with regularization phase continues for 16 epochs with batch size = 100, $\eta = 2.5e - 05$ and $\lambda = 2.22e - 07$. Evaluations on the validation set is done every 6000 steps (24 times each epoch) with BLEU lower-bound = 27.3 and pruning 1% of the remaining weights when required. Finally we finetune without regularization for 5 more epochs. With respect to [25], we stop pruning when the

²<https://huggingface.co/>

Table 6 Example of translation pairs from En-De WMT14.

Source	Translation
Iron cement protects the ingot against the hot, abrasive steel casting process.	Nach der Aushärtung schützt iron cement die Kokille gegen den heissen, abrasiven Stahlguss.
Goods and services advancement through the P.O.Box system is NOT ALLOWED.	der Vertrieb Ihrer Waren und Dienstleistungen durch das Postfach System WIRD NICHT ZUGELASSEN.
Their achievement remains one of the greatest in recent history.	Das bleibt eine der größten Errungenschaften in der jüngeren Geschichte.

Table 7 Dialog sample from Taskmaster-1.

Input	Target
<user>Hi there, could you please help me with an order of Pizza?<enduser> <agent>Sure, where would you like to order you pizza from?<endagent> <user>I would like to order a pizza from Domino’s.<enduser> <agent>What kind of pizza do you want to order? <endagent> <user>What are the specials they have right now? <enduser> <agent>There are family and party combos currently on offer <endagent > <user>No, I just want a large pizza <enduser> <agent>They have any large specialty pizza for 10.99 <endagent> <user>What are their specialty pizzas? <enduser>	<agent>Well, there is the Extravagazza, Meatzza, Philly Cheesesteak, Hawaiian, Buffalo Chicken Ranch, and more. Would you like to hear more? <endagent>

Table 8 Transformer hyperparameters.

Hyperparameters	Taskmaster-1	WMT14
vocabulary	32k	32k
# encoder layers	2	6
# decoder layers	2	6
# attention heads	4	8
feed forward dim	256	2048
embedding dim.	256	512
# weights	10M	61M
max sequence len.	256	256
beam size	6	4
length penalty	-	0.6

validation performance reaches a plateau (or drop) and never re-climb the user-defined lower-bound, as described in Section 4. This criterion causes the pruning to stop at $\sim 80\%$ of sparsity.

As can be seen from figure 1, our pruning technique performs better than all other methods, preserving BLEU values up to $\sim 75\%$ of sparsity while dropping at most 0.5 points with respect to the baseline.

It also seems to be more resilient at higher compression levels since BLEU scores start to degrade visibly only after $\sim 75\%$ of sparsity is reached, whereas the other five pruning methods degrade earlier.

Table 9 shows in detail layer-by-layer and global pruning percentages at the higher compression level reached. Table 10 shows the disk space occupied by the pruned and unpruned model after being compressed using GZIP³ and BZIP2⁴ algorithms with two different compression rates, identified by -1 and -9. In particular we can see that using BZIP2 the pruned model is 4 times smaller on disk than the unpruned one.

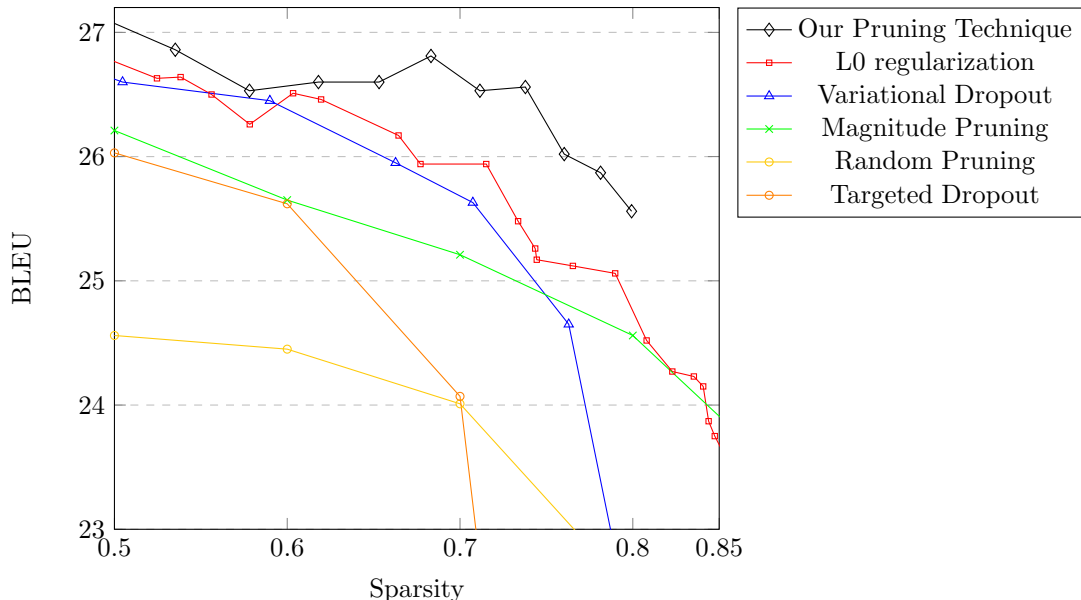


Fig. 1 BLEU results comparison at different sparsity levels on WMT14 dataset. Except for our technique, the datapoints are taken from [19] for targeted dropout and from [25] for the others methods, for which we take only their best runs (in terms of BLEU).

Table 9 Layer-by-layer and global pruning results on WMT14.

Model	Residual Weights (%)					BLEU	Sparsity (%)
	Encoder Attention	Decoder Attention	Encoder FFN	Decoder FFN	Embedding/ Classification Head		
Baseline	100	100	100	100	100	27.20	–
Our model	24.70	27.54	21.27	20.10	12.43	25.56	79.93

Table 10 Disk space dimensions of pruned/unpruned Transformer models on WMT14.

Model	GZIP		BZIP2	
	GZIP -1	GZIP -9	BZIP2 -1	BZIP2 -9
Unpruned	228.9 MB	228.3 MB	237.1 MB	233.2 MB
Pruned	87.2 MB	66.8 MB	59.9 MB	58.2 MB

6.3 Transformer on Taskmaster-1

Following [41] we use as input-data the dialog context up to the last user turn, and as target the subsequent assistant utterance. An example of this format is shown in table 7.

Transformer architecture details are presented in [41], and shown in table 8. We train it for 15 epochs using the Adam optimizer ($\beta_1 =$

$0.85, \beta_2 = 0.997, eps = 1e - 8$) with batch size = 150 and dropout = 0.2. The final checkpoint we obtain shows comparable BLEU performance to the author’s one.

Starting from this checkpoint, we finetune with regularization for 40 epochs with $\eta = 0.0005$. We rely on a small $\lambda = 1e - 05$ not to lose performance during the early stages. We find that checking every 300 training steps (i.e. 4 times every epoch) is a good compromise to get frequent pruning steps while retaining generation ability. The BLEU lower-bound is set to 6.03, which is very close to the author’s baseline result of 6.11, and the pruning-percentage is 0.1. After 30 epochs, the algorithm makes the last pruning, and the last 10 epochs are used to recover BLEU score.

³more info at: <https://www.gnu.org/software/gzip/>

⁴more info at: <https://www.sourceware.org/bzip2/>

Table 11 Layer by layer and global pruning outcomes on Taskmaster-1.

Model	Residual Weights (%)					BLEU	Sparsity (%)
	Encoder Attention	Decoder Attention	Encoder FFN	Decoder FFN	Embedding/ Classification Head		
Baseline	100	100	100	100	100	6.11	–
L1	2.53	18.57	1.17	53.08	20.99	6.15	79.49
L2	17.71	21.20	15.21	26.61	6.28	6.15	90.10
Our model	21.53	21.77	21.68	26.93	7.12	6.21	90.09

Table 12 Disk space dimensions of pruned/unpruned Transformer models on TSK-1.

Model	GZIP		BZIP2	
	GZIP -1	GZIP -9	BZIP2 -1	BZIP2 -9
Unpruned	40.2 MB	40.1 MB	41.7 MB	41.1 MB
Pruned	11.2 MB	7.4 MB	6.4 MB	6.2 MB

To the best of our knowledge there are no achievements yet in literature about weights sparsity in dialog generation tasks. We therefore establish in this context the first results, resumed in table 11, testing our method against L1 and L2 regularization baselines.

Our sparsification technique allows to obtain a highly sparsified model, with a sparsity level greater than 90%. Moreover, our final BLEU is even higher than the original result, suggesting that in some cases a sparsified model is able to generalize better than a non sparsified one.

Table 12 shows the disk space occupied by the pruned and unpruned model after being compressed. Also in this case very good compressions can be achieved. In particular using BZIP2 the pruned model is about 6,6 times smaller on disk than the unpruned one.

7 Conclusions

The identification of irrelevant model’s parameters for pruning is the focal point of this work. We propose a solution which is an improvement of classical weight decay and consequently suitable for any loss functional. Moreover, it is simple to implement and results in a largely usable and general framework which proves to be effective in sparsifying different deep architectures.

We reach state-of-the-art results in two out of four Image Classification datasets and improve state-of-the-art for the others in terms of the combination of sparsity and accuracy, also getting a

new state-of-the-art in the machine translation dataset WMT14. Since there are very few results for sparsity in language generation tasks, another contribution of this paper is that we give a new datapoint on Taskmaster-1.

A future interesting contribution could be to explore applications of our method to low resource devices like smartphones and IOT systems.

Acknowledgments. This research has been partially carried on in the context of the Visiting Professor Program of the Italian Istituto Nazionale di Alta Matematica (INdAM).

References

- [1] K. Zhang, L. V. Gool, R. Timofte, Deep unfolding network for image super-resolution, in: IEEE/CVF Conference on Computer Vision and Pattern Recognition (CVPR), 2020.
- [2] T. He, Z. Zhang, H. Zhang, Z. Zhang, J. Xie, M. Li, Bag of tricks for image classification with convolutional neural networks, in: Proceedings of the IEEE/CVF Conference on Computer Vision and Pattern Recognition (CVPR), 2019.
- [3] K. He, X. Zhang, S. Ren, J. Sun, Deep residual learning for image recognition, 2016, pp. 770–778.
- [4] K. Simonyan, A. Zisserman, Very deep convolutional networks for large-scale image recognition, in: International Conference on Learning Representations, 2015.
- [5] C. Szegedy, W. Liu, Y. Jia, P. Sermanet, S. Reed, D. Anguelov, D. Erhan, V. Vanhoucke, A. Rabinovich, Going deeper with convolutions, in: 2015 IEEE Conference on

Computer Vision and Pattern Recognition (CVPR), 2015, pp. 1–9.

- [6] L. Guo, J. Liu, X. Zhu, P. Yao, S. Lu, H. Lu, Normalized and geometry-aware self-attention network for image captioning, in: IEEE/CVF Conference on Computer Vision and Pattern Recognition (CVPR), 2020.
- [7] Y. Feng, L. Ma, W. Liu, J. Luo, Unsupervised image captioning, in: Proceedings of the IEEE/CVF Conference on Computer Vision and Pattern Recognition (CVPR), 2019.
- [8] R. Puduppully, L. Dong, M. Lapata, Data-to-text generation with content selection and planning, in: The Thirty-Third AAAI Conference on Artificial Intelligence, AAAI 2019, The Thirty-First Innovative Applications of Artificial Intelligence Conference, IAAI 2019, The Ninth AAAI Symposium on Educational Advances in Artificial Intelligence, EAAI 2019, Honolulu, Hawaii, USA, January 27 - February 1, 2019, 2019, pp. 6908–6915.
- [9] O. Dusek, J. Novikova, V. Rieser, Evaluating the state-of-the-art of end-to-end natural language generation: The E2E NLG challenge, *Comput. Speech Lang.* 59 (2020) 123–156.
- [10] D. W. Otter, J. R. Medina, J. K. Kalita, A survey of the usages of deep learning in natural language processing, *CoRR* abs/1807.10854 (2018).
- [11] H. Mei, M. Bansal, M. R. Walter, What to talk about and how? selective generation using lstms with coarse-to-fine alignment, in: NAACL HLT 2016, The 2016 Conference of the North American Chapter of the Association for Computational Linguistics: Human Language Technologies, San Diego California, USA, June 12-17, 2016, 2016, pp. 720–730.
- [12] A. Vaswani, N. Shazeer, N. Parmar, J. Uszkoreit, L. Jones, A. N. Gomez, L. Kaiser, I. Polosukhin, Attention is all you need, 2017.
- [13] D. Bahdanau, K. Cho, Y. Bengio, Neural machine translation by jointly learning to align and translate, in: 3rd International Conference on Learning Representations, ICLR 2015, San Diego, CA, USA, May 7-9, 2015, Conference Track Proceedings, 2015.
- [14] S. Han, J. Pool, J. Tran, W. J. Dally, Learning both weights and connections for efficient neural network, in: C. Cortes, N. D. Lawrence, D. D. Lee, M. Sugiyama, R. Garnett (Eds.), *Advances in Neural Information Processing Systems 28: Annual Conference on Neural Information Processing Systems 2015*, December 7-12, 2015, Montreal, Quebec, Canada, 2015, pp. 1135–1143.
- [15] K. Ullrich, E. Meeds, M. Welling, Soft weight-sharing for neural network compression, in: 5th International Conference on Learning Representations, ICLR 2017, Toulon, France, April 24-26, 2017, Conference Track Proceedings, OpenReview.net, 2017.
- [16] Liu, J., Wang, Y., Qiao, Y. (2017, February). Sparse deep transfer learning for convolutional neural network. In *Thirty-First AAAI Conference on Artificial Intelligence*.
- [17] E. Tartaglione, S. Lepsø y, A. Fiandrotti, G. Francini, Learning sparse neural networks via sensitivity-driven regularization, in: S. Bengio, H. Wallach, H. Larochelle, K. Grauman, N. Cesa-Bianchi, R. Garnett (Eds.), *Advances in Neural Information Processing Systems*, Vol. 31, Curran Associates, Inc., 2018.
- [18] E. Tartaglione, A. Bragagnolo, A. Fiandrotti, M. Grangetto, Loss-based sensitivity regularization: towards deep sparse neural networks (2020).
- [19] A. N. Gomez, I. Zhang, K. Swersky, Y. Gal, G. E. Hinton, Learning sparse networks using targeted dropout, *CoRR* abs/1905.13678 (2019).
- [20] M. D. Collins, P. Kohli, Memory bounded deep convolutional networks (2014).
- [21] D. Molchanov, A. Ashukha, D. P. Vetrov, Variational dropout sparsifies deep neural networks, in: D. Precup, Y. W. Teh (Eds.), *Proceedings of the 34th International Conference on Machine Learning, ICML 2017*,

Sydney, NSW, Australia, 6-11 August 2017, Vol. 70 of Proceedings of Machine Learning Research, PMLR, 2017, pp. 2498–2507.

- [22] H. Salehinejad, S. Valaee, Edropout: Energy-based dropout and pruning of deep neural networks, CoRR abs/2006.04270 (2020).
- [23] N. Lee, T. Ajanthan, P. H. S. Torr, Snip: single-shot network pruning based on connection sensitivity, in: 7th International Conference on Learning Representations, ICLR 2019, New Orleans, LA, USA, May 6-9, 2019, OpenReview.net, 2019.
- [24] Y. Guo, A. Yao, Y. Chen, Dynamic network surgery for efficient dnns, in: D. D. Lee, M. Sugiyama, U. von Luxburg, I. Guyon, R. Garnett (Eds.), Advances in Neural Information Processing Systems 29: Annual Conference on Neural Information Processing Systems 2016, December 5-10, 2016, Barcelona, Spain, 2016, pp. 1379–1387.
- [25] T. Gale, E. Elsen, S. Hooker, The state of sparsity in deep neural networks, CoRR abs/1902.09574 (2019).
- [26] C. Louizos, M. Welling, D. P. Kingma, Learning sparse neural networks through l₀ regularization, in: 6th International Conference on Learning Representations, ICLR 2018, Vancouver, BC, Canada, April 30 - May 3, 2018, Conference Track Proceedings, OpenReview.net, 2018.
- [27] V. Badeva, V. Morozov, Problèmes incorrectement posés: Théorie et applications en identification, filtrage optimal, contrôle optimal, analyse et synthèse de systèmes, reconnaissance d'images, Série Automatique, Masson, 1991.
- [28] I. J. Goodfellow, Y. Bengio, A. C. Courville, Deep Learning, Adaptive computation and machine learning, MIT Press, 2016.
- [29] A. N. Tikhonov, Solution of incorrectly formulated problems and the regularization method, Soviet Math. Dokl. 4 (1963) 1035–1038.
- [30] A. Tikhonov, V. Arsenin, Solutions of ill-posed problems, Scripta series in mathematics, Winston, Washington DC, 1977.
- [31] K. Papineni, S. Roukos, T. Ward, W. J. Zhu, Bleu: a method for automatic evaluation of machine translation (10 2002).
- [32] Y. LeCun, C. Cortes, MNIST handwritten digit database (1990).
- [33] H. Xiao, K. Rasul, R. Vollgraf, Fashion-mnist: a novel image dataset for benchmarking machine learning algorithms, CoRR abs/1708.07747 (2017).
- [34] V. N. Alex Krizhevsky, G. Hinton, CIFAR RGB image dataset (2009).
- [35] A. Torralba, R. Fergus, W. T. Freeman, 80 million tiny images: A large data set for nonparametric object and scene recognition, IEEE Transactions on Pattern Analysis and Machine Intelligence 30 (11) (2008) 1958–1970.
- [36] J. Deng, W. Dong, R. Socher, L.-J. Li, K. Li, L. Fei-Fei, Imagenet: A large-scale hierarchical image database, in: 2009 IEEE conference on computer vision and pattern recognition, Ieee, 2009, pp. 248–255.
- [37] G. A. Miller, Wordnet: A lexical database for english, Commun. ACM 38 (11) (1995) 39–41.
- [38] Y. LeCun, B. Boser, J. S. Denker, D. Henderson, R. E. Howard, W. Hubbard, L. D. Jackel, Backpropagation applied to handwritten zip code recognition, Neural Computation 1 (4) (1989) 541–551.
- [39] P. Michel, O. Levy, G. Neubig, Are sixteen heads really better than one?, in: H. Wallach, H. Larochelle, A. Beygelzimer, F. d'Alché-Buc, E. Fox, R. Garnett (Eds.), Advances in Neural Information Processing Systems, Vol. 32, Curran Associates, Inc., 2019.
- [40] E. Voita, D. Talbot, F. Moiseev, R. Senrich, I. Titov, Analyzing Multi-Head Self-Attention: Specialized Heads Do the Heavy

- Lifting, the Rest Can Be Pruned, in: Proceedings of the 57th Annual Meeting of the Association for Computational Linguistics, Association for Computational Linguistics, Stroudsburg, PA, USA, 2019, pp. 5797–5808.
- [41] B. Byrne, K. Krishnamoorthi, C. Sankar, A. Neelakantan, B. Goodrich, D. Duckworth, S. Yavuz, A. Dubey, K. Kim, A. Cedilnik, Taskmaster-1: Toward a realistic and diverse dialog dataset, in: K. Inui, J. Jiang, V. Ng, X. Wan (Eds.), Proceedings of the 2019 Conference on Empirical Methods in Natural Language Processing and the 9th International Joint Conference on Natural Language Processing, EMNLP-IJCNLP 2019, Hong Kong, China, November 3-7, 2019, Association for Computational Linguistics, 2019, pp. 4515–4524.
- [42] O. Bojar, C. Buck, C. Federmann, B. Haddow, P. Koehn, J. Leveling, C. Monz, P. Pecina, M. Post, H. Saint-Amand, R. Soricut, L. Specia, A. Tamchyna, Findings of the 2014 workshop on statistical machine translation, in: Proceedings of the Ninth Workshop on Statistical Machine Translation, Association for Computational Linguistics, Baltimore, Maryland, USA, 2014, pp. 12–58.
- [43] P. Koehn, Europarl: A Parallel Corpus for Statistical Machine Translation, in: Conference Proceedings: the tenth Machine Translation Summit, AAMT, AAMT, Phuket, Thailand, 2005, pp. 79–86.
- [44] J. Tiedemann, Parallel data, tools and interfaces in opus, in: N. C. C. Chair), K. Choukri, T. Declerck, M. U. Dogan, B. Maegaard, J. Mariani, J. Odijk, S. Piperidis (Eds.), Proceedings of the Eight International Conference on Language Resources and Evaluation (LREC’12), European Language Resources Association (ELRA), Istanbul, Turkey, 2012.
- [45] CommonCrawl, CommonCrawl’s dataset (2012).
- [46] T. S. N. L. P. Group, Neural Machine Translation (2015).